AIAA 96-4046
Dependence of Optimum Structural Weight on Aerodynamic Shape for a High-Speed Civil Transport

V. Balabanov, M. Kaufman, D.L. Knill,
A.A. Giunta, B. Grossman, W.H. Mason,
and L.T. Watson
Virginia Polytechnic Institute and
State University, Blacksburg, VA 24061

and

R.T. Haftka
University of Florida
Gainesville, FL 32611-6250

6th AIAA/NASA/ISSMO
Symposium on Multidisciplinary
Analysis and Optimization
September 4-6, 1996 / Bellevue, WA

DEPENDENCE OF OPTIMAL STRUCTURAL WEIGHT ON AERODYNAMIC SHAPE FOR A HIGH SPEED CIVIL TRANSPORT

V. Balabanov*, M. Kaufman*, D. L. Knill*, D. Haim†, O. Golovidov*, A. A. Giunta*
Multidisciplinary Analysis and Design (MAD) Center for Advanced Vehicles
Virginia Polytechnic Institute and State University
Mail Stop 0203, Blacksburg, Virginia 24061

Raphael T. Haftka‡,
Department of Aerospace Engineering, Mechanics and Engineering Science, University of Florida
Gainesville, Florida 32611-6250

B. Grossman§, W.H. Mason¶ and L.T. Watson#
MAD Center for Advanced Vehicles, Virginia Tech

Abstract

A procedure for generating a customized weight function for wing bending material weight of the High Speed Civil Transport (HSCT) is described. The weight function is based on the shape parameters. A response surface methodology is used to fit a quadratic polynomial to data gathered from a large number of structural optimizations. The results of the structural optimization are noisy. Noise reduction in the structural optimization results is discussed. Several techniques are used to minimize the number of required structural optimizations and to maintain accuracy. Simple analysis techniques are used to find regions of the design space where reasonable HSCT designs could occur, thus customizing the weight function to the design requirements of the HSCT, while the response surfaces themselves are created employing detailed analysis methods. Intervening variables and analysis of variance are used to reduce the number of polynomial terms in the response surface model functions. Minimum variance and minimum bias procedures for creation of response surfaces are compared. Configuration optimization of the HSCT employing customized weight functions with different response surfaces are compared.

1. Introduction

The design of a High Speed Civil Transport (HSCT) configuration is an active research topic at the Multidisciplinary Analysis and Design (MAD) Center for Advanced Vehicles at Virginia Tech. Our design goal is to minimize takeoff gross weight for a range of 5500 nautical miles, a cruise Mach number of 2.4, while carrying 251 passengers. We have developed a model that completely defines the HSCT design problem using twenty-eight design variables. Twenty-five of the design variables describe the geometry of the aircraft, and three variables describe an idealized cruise mission and fuel weight [1,2].

In the conceptual and preliminary design phases statistically-derived, experience-based algebraic models, known as weight functions or weight equations, are often used to estimate weights of all components. However, these weight functions may not accurately predict weights of some components of relatively new conceptual designs, such as HSCT, because they are derived mainly from existing aircraft data.

As a part of the configuration optimization, we estimate structural weight using an algebraic weight function (weight equation) from the Flight Optimization System (FLOPS) [3]. Previous studies showed good correlation for structural weight prediction between FLOPS and structural optimization [4]. However, work by Huang *et al.*[4] also indicated that the FLOPS weight equation may not be accurate in estimating wing bending material weight, when it is necessary to take into account planform shape changes. Consequently, we

* Graduate Research Assistant, Dept. of Aerospace & Ocean Eng., Student Member AIAA
† Graduate Research Assistant, Dept. of Computer Sci. and Math.
‡ Professor, Associate Fellow AIAA
§ Professor, Dept. Head, Dept. of Aerospace & Ocean Eng., Associate Fellow AIAA
¶ Professor, Dept. of Aerospace & Ocean Eng., Associate Fellow AIAA
# Professor, Dept. of Computer Sci. and Math.

have been working on the implementation of structural optimization for estimating structural bending material weight into the configuration optimization.

One may consider complete coupling of the structural optimization with the configuration optimization process. However, this approach is difficult for several reasons. First, the wing bending material weight obtained as a result of structural optimization is not a smooth function of the configuration design variables. This is due to changes in the set of active constraints as the configuration changes and numerical noise which includes incomplete convergence of the structural optimization as well as noise in the aerodynamic loads. Therefore, a derivative-based optimization would be difficult to perform. Second, the configuration design process requires structural weight information at a large number of design points and one does not know beforehand for which points in the design space structural optimization should be performed. These points are determined by the optimizer performing the configuration optimization. The difficulties described above and the expense of structural optimization make complete coupling of the structural optimization with the configuration optimization process unrealistic for HSCT design.

Coupling unrelated optimization processes also introduces code integration problems. Different optimization software packages utilize different design variables, input parameters, and output formats. Additional software could be developed to automate code interaction. However, this is rarely a straightforward process. Moreover, such software produces inefficiencies on modern high performance computers.

The objective of this paper is to investigate the noisy behavior of the structural weight computed by structural optimization and to describe a response surface approach that may be used to filter out this noise. Instead of performing structural optimization during the configuration design process, structural optimization is performed for a large number of aircraft geometries beforehand. Results of the structural optimizations are then used to create a response surface to the wing bending material weight. Since the geometries are based on the configuration design variables, code integration problems are eliminated.

While one desires accurate results throughout the entire design space, it is impractical to perform structural optimization for every conceivable HSCT configuration. For this reason, techniques are developed to limit the design space domain and to balance the response surface accuracy with development cost. These methods are not specific to the wing bending material weight and can be applied to many response surface applications.

Several approaches were tried in order to reduce the cost of generating the response surface. First, a previously developed statistical weight function was used to identify a small set of geometric and loading parameters which characterize the wing bending material weight objective function. This reduced set of variables was then employed to reduce the dimension of the model function. Second, simple analysis techniques were used to identify a reasonable design space where the optimum design may be located. Finally, a fixed number of reasonable designs were picked using statistical *design of experiments* techniques to produce response surfaces that reflect the entire reasonable design space. Only at these designs were structural optimizations performed.

The large number of structural optimizations required make this problem especially suitable for coarse grain parallelization. A finite-element-based structural optimization code GENESIS[5], was used to optimize the design configurations. A coarse-grain parallelization of GENESIS on the Intel *Paragon* yielded reasonable speedups and greatly accelerated the creation of the response surface.

By its nature, the response surface is a simple algebraic expression that provides smooth derivative information. Although initially expensive to establish, the surface uses minimal resources once implemented. This makes it ideal for the HSCT design problem. To demonstrate the response surfaces' suitability to design, optimizations of the HSCT configurations are performed. Results are presented with and without the implementation of the response surface.

This paper is a direct continuation of the work presented in Refs. 6 and 7. The problem discussed in the present paper was first formulated and solved in Ref. 6, where Kaufman *et al.* described in details its statistical and computational aspects. It was found there that structural optimization data used for creation of the response surface was noisy, but the origin of the noise was not identified. Reference 7 described structural aspects of the problem in more detail and identified the major source of the noise as coming from aerodynamic loading. However, the noise was not reduced significantly. In the present paper the aerodynamic noise is traced to the camber optimization of the wing and results with substantial less noise are obtained. Accuracy of the response surfaces with and without noise are compared. Additionally, two alternative *design of experiment* techniques for selecting configurations for structural optimization are compared. Results of HSCT optimization using the alternative response surfaces are also compared.

2. HSCT Design Problem

In research conducted by members of the Multidisciplinary Analysis and Design (MAD) Center for Advanced Vehicles at Virginia Tech, the design problem is the optimization of an HSCT configuration to minimize takeoff gross weight (TOGW) for a range of 5500

nautical miles and a cruise Mach number of 2.4, while carrying 251 passengers. The choice of gross weight as the objective function directly incorporates both aerodynamic and structural considerations, in that the structural design directly affects aircraft empty weight and drag, while aerodynamic performance dictates the drag and thus the required fuel weight. Trim and control requirements are also explicitly treated.

To successfully perform aircraft configuration optimization it is very important to have a simple, but meaningful mathematical characterization of the geometry of the aircraft. Our design group at Virginia Tech has developed a model that completely defines the HSCT design problem using twenty-eight design variables (listed in Table 1).

Table 1. HSCT design variables and baseline values.

Number	Value	Description
1	181.48	Wing root chord (ft)
2	155.9	LE break point, x (ft)
3	49.2	LE break point, y (ft)
4	181.6	TE break point, x (ft)
5	64.2	TE break point, y (ft)
6	169.5	LE wing tip, x (ft)
7	7.00	Wing tip chord (ft)
8	75.9	Wing semi-span (ft)
9	0.40	Chordwise max. t/c location
10	3.69	LE radius parameter
11	2.58	Airfoil t/c at root (%)
12	2.16	Airfoil t/c at LE break (%)
13	1.80	Airfoil t/c at tip (%)
14	2.20	Fuselage restraint 1, x (ft)
15	1.06	Fuselage restraint 1, r (ft)
16	12.20	Fuselage restraint 2, x (ft)
17	3.50	Fuselage restraint 2, r (ft)
18	132.46	Fuselage restraint 3, x (ft)
19	5.34	Fuselage restraint 3, r (ft)
20	248.67	Fuselage restraint 4, x (ft)
21	4.67	Fuselage restraint 4, r (ft)
22	26.23	Nacelle 1, y (ft)
23	33.09	Nacelle 2, y (ft)
24	322,617	Mission fuel (lbs)
25	64,794	Starting cruise altitude (ft)
26	33.90	Cruise climb rate (ft/min)
27	697.9	Vertical tail area (ft^2)
28	713.0	Horizontal tail area (ft^2)

Twenty-five of the design variables describe the geometry of the aircraft and can be divided into five categories: wing planform, airfoil shape, tail areas, nacelle placement, and fuselage shape. In addition to the geometric parameters, three variables define the idealized cruise mission. One variable is the mission fuel and the other two are initial cruise altitude and the constant climb rate used in the range calculation. No design variables are used to describe the camber distribution. Instead, camber is generated by Carlson's program WINGDES[8].

In this study, a baseline HSCT is used to provide a point near the interior of the feasible design space. The baseline geometry is the one that was thought to be optimal previously[9], (Table 1). Because of modifications and improvements to our analysis methods, this geometry no longer satisfies all of the performance constraints. However, more recent optimal designs show similar characteristics.

Table 2. Constraints on the HSCT design.

Number	Description
1	Range $\geq$ 5,500 nmi
2	Landing angle of attack $\leq 12^\circ$
3	C_L at landing speed ≤ 1.0
4-21	Landing section $C_L \leq 2.0$
22	Fuel volume $\leq$ 50% wing volume
23-40	Wing chord ≥ 7.0 ft
41	LE break, $y \leq$ wing semi span
42	TE break, $y \leq$ wing semi span
43	Root chord t/c $> 1.5\%$
44	LE break chord $t/c > 1.5\%$
45	TE break chord $t/c > 1.5\%$
46	Fuselage: $x_r est_1 \geq 5$ ft
47	Fuselage: $x_r est_1 + 10ft \leq x_r est_2$
48	Fuselage: $x_r est_2 + 10ft \leq x_r est_3$
49	Fuselage: $x_r est_3 + 10ft \leq x_r est_4$
50	Fuselage: $x_r est_4 + 10ft \leq 300ft$
51	Nacelle 1, $y \geq$ side-of-body
52	Nacelle 1, $y \leq$ nacelle 2, y
53	Engine out stability criterion
54	Minimum airfoil section spacing at wing tip
55-56	No engine scrape at landing angle-of-attack
57-58	No engine scrape at landing angle-of-attack, with 5° roll
59	No wing tip scrape at landing angle-of-attack, with 5° roll
60	No wing trailing-edge break point at landing, with 5° roll
61	Crosswind landing capability with aileron deflection only
62	Crosswind landing capability with aileron and rudder deflection
63	Rudder deflection $\leq 22.5^\circ$
64	Takeoff rotation must occur prior to reaching 90% of takeoff velocity
65	Root trailing-edge must not overlap root leading-edge of horizontal tail
66-67	Required engine thrust $\leq$ available thrust

Sixty-seven geometry, performance, and aerodynamic constraints are included in the optimization. They are necessary to prevent the optimizer from creating physically meaningless designs. Aerodynamic and performance constraints can only be assessed after a complete analysis of the HSCT design; however, the geometric constraints can be evaluated using algebraic relations based on 28 design variables. Thus we get the opportunity to efficiently identify reasonable designs from the point of view of planform geometry, eliminating nonsensical designs where, for example, tip chord of the wing is greater than root chord. The geometric, performance and aerodynamic constraints are listed in Table 2. More details are presented in Refs. 4, 10.

3. Structural Modeling

The goal of performing structural optimization is to provide wing bending material weight to be used later in the overall multidisciplinary optimization process. Due to the large number of optimizations that must be performed to create a response surface, a relatively simple structural optimization model was used. We employed a structural model of the HSCT with a fixed arrangement of spars and ribs. The wing and fuselage skin were modeled by membrane elements. Spar and rib caps were modeled by rod elements. Vertical rods and shear panels were used to model spar and rib webs. Because of symmetry, we only generate a finite element model of half the aircraft. The typical finite element (FE) model is made up of 923 elements jointed at 193 nodes with 579 total degrees of freedom (Fig. 1).

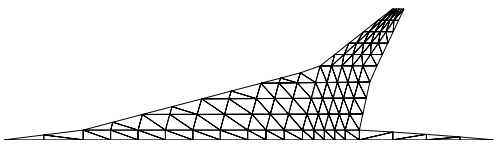

Figure 1. Finite element model of HSCT.

Forty design variables were used for the structural optimization, including 26 to define skin panel thicknesses, 12 for spar cap areas and 2 design variables were used for the rib caps areas. A uniform area and thickness distribution was assumed for elements controlled by one design variable.

We apply stress constraints based on Von Mises yield criterion to each panel, spar, and rib cap element. In addition, local buckling constraints were applied. Because of the coarseness of the model, we only employed it to estimate the bending material weight of the structure, and continued to use FLOPS weight equations to estimate other parts of the structural and nonstructural weight. Following the FLOPS weight equation breakdown, the bending material weight was defined to consist mostly of the weight of the spar caps and skin panels. It accounts for about 4.5% of the gross takeoff weight. However, the entire wing structural weight was the objective function of the structural optimization. After optimization was performed, wing bending material weight was calculated based on thickness of specific portions of the wing.

A special mesh generator was implemented to automatically create a finite element model based on the twenty-eight HSCT design variables. This mesh generator created the finite element nodes and element topology data, estimated the location of non-structural weights, and predicted the geometry of the wing fuel tanks. Fuel was assumed to be stored in thirty-one tanks throughout the aircraft.

The loads applied to the structural model were composed of the aerodynamic and inertia forces. Inertia loads represented the combined effects of non-structural items, fuel weight, and the distributed weight of the structure. Aerodynamic loads for supersonic flight conditions were determined using a supersonic panel method, and loads for subsonic flight conditions were from a vortex-lattice method. The structure was assumed to be rigid for the determination of aerodynamic forces. Previous studies indicated that structural flexibility did not have a large effect on the structural wing weight (objective function of the structural optimization) for this particular configuration [4,11]. For each design, orientation of the aerodynamic loads was governed by camber distributions generated by Carlson's program WINGDES [8]. A surface spline interpolation method was used to translate forces between aerodynamic node and structural node locations. Five load cases were considered for the structural optimization (Table 3). More details about loads can be found in Ref. 4.

Table 3. Load cases for the structural optimization.

Load case	Mach number	Load factor	Altitude (ft.)	% of fuel
1	2.4	1.0	63175	50
2	1.2	1.0	29670	90
3	0.6	2.5	10000	95
4	2.4	2.5	56949	80
5	0.0	1.5	0	100

4. Coarse Grain Parallelization

Due to large number of design variables, the number of structural optimizations needed to be performed beforehand is more than a thousand. To efficiently perform such a large number of structural optimizations we took advantage of coarse grain parallel computing.

Coarse grain parallelization implies that multiple structural optimizations for multiple HSCT designs, are performed simultaneously on separate processors.

Each processor maintains its own data, so that interaction between the processors is minimal. We organized the parallel computation in a *"slave-master"* paradigm, with one processor free of computational work. This processor (the master) copies input and output files for the rest of processors (the slaves), checks which processors have finished their work, and assigns new jobs to them. A twenty-eight node Intel *Paragon* was used for this work.

As the number of processors is increased on a distributed memory architecture machine like the Intel *Paragon*, disk input/output (I/O) limits the efficiency of the parallel computations. This factor was the primary basis for choosing the GENESIS finite element structural optimization code for implementation in the parallel environment. GENESIS was available from the developer in a reduced I/O form and thus made it an effective code to use on the *Paragon*. GENESIS provides three different optimization methods: method of feasible directions (FDM), sequential linear programming (SLP) and sequential quadratic programming (SQP). We used method of feasible directions for our problem.

Figure 2 shows the benefits of the reduced I/O version of GENESIS. The speedups of a parallel computation is defined as T_s/T_p where T_s is the serial execution time and T_p is the parallel execution time using p processors. In an ideal situation, speedup would be equal to the number p of processors being used. With the standard version, maximum speedup levels off at 2.3, regardless of the number of processors, while the reduced I/O version achieves a speedup of 11.7 using 20 processors. This is still rather poor, showing a need for further reduction of I/O.

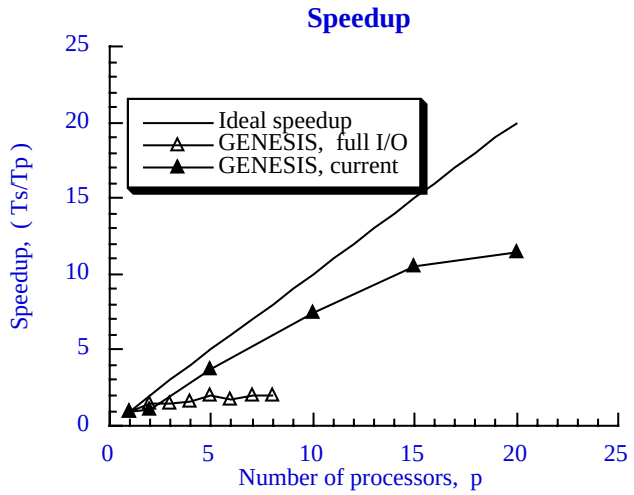

Figure 2. Ideal versus actual speedup for parallel execution of GENESIS.

5. Noise in the Structural Optimization Results

Unfortunately, the weight obtained by structural optimization is not a smooth function of the configuration design variables. This nonsmoothness is the result of changes in the set of active constraints as the configuration changes and numerical noise which includes incomplete convergence of the structural optimization as well as noise in the aerodynamic loads.

5.1 Design-line plots

A procedure which we use to detect noise in a response quantity is to plot the response along a straight line segment in design space. This plot is sometimes called an α plot [12]. The segment is obtained by connecting two close design points:

$$\mathbf{x} = (1-\alpha)\mathbf{x_s} + \alpha\mathbf{x_f} \ , \quad 0 \le \alpha \le 1$$

where $\mathbf{x_s}$ is the vector of starting design variables, $\mathbf{x_f}$ is the vector of final design variables.

In order to check the amount of noise in the results of the structural optimization, two close, conventionally looking HSCT designs are chosen as the endpoints of the segment. These designs are referred to as Design #1 and Design #20 (shown in the Figure 3).

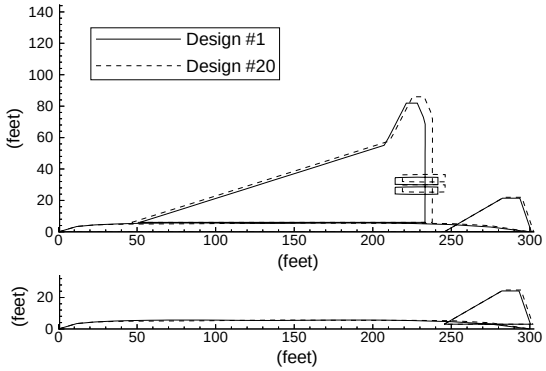

Figure 3. First and last designs in α plot

The configuration design variables which define these two designs differ by about 3%. Eighteen additional equally spaced designs are taken along the straight line segment connecting two endpoint designs.

Figure 4 shows the initially obtained variation in the wing bending material weight from structural optimization for the 20 designs. It appears from the figure that the noise in the structural optimization weight is on the order of 20–30%.

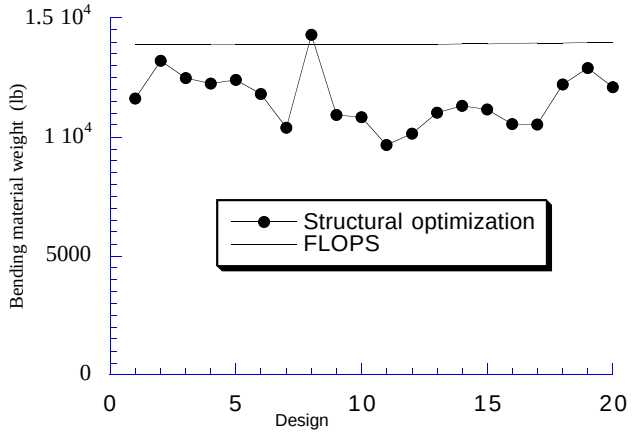

Figure 4. Initial noise in wing bending material weight.

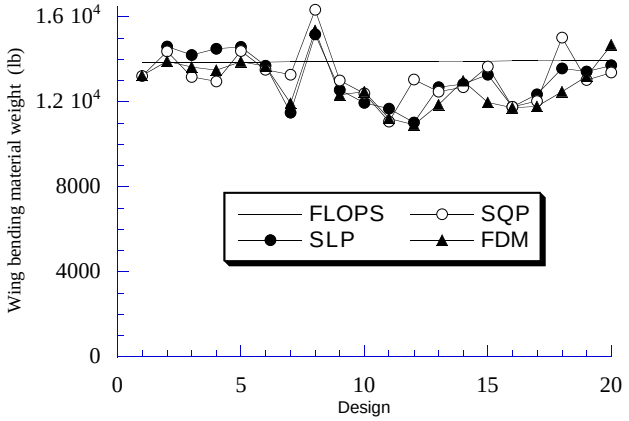

Figure 5. Wing bending material weight from different structural optimization methods.

5.2 Reduction of noise

We first explored the possibility that most of the noise in the optimization results was due to unconverged optimization results. Accordingly we tried reducing move limits and tightening convergence criteria. Move limits were reduced from 30% to 10% and stopping convergence criteria were reduced from 1% to 0.1%. This had a favorable but small effect. The noise was reduced from 30% to about 29%. We looked for other optimization related noise sources and found that one of the possible sources was the objective function of the structural optimization (total wing structural weight). We found that the total wing structural weight varied less erratically than the bending material weight which was extracted from it. Apparently, the optimization procedure could find designs with very similar total weight, but with different distributions between the component defined as the bending material by FLOPS and the rest of the weight. Consequently, the optimization procedure converged to designs with similar total weights as we changed the aerodynamic shape, but different bending-material weights. To overcome this difficulty we tried to make the objective function of the structural optimization closer to the definition of the wing bending material weight: we relaxed stress and buckling constraints for the portions of the wing whose weight was not included into wing bending material weight. Thus, we assumed that structural arrangement of these portion of the wing should be given. This manipulation of the objective function reduced the noise by another 2%.

We also tried three different optimization methods with GENESIS: method of feasible directions (FDM), sequential linear programming (SLP) and sequential quadratic programming (SQP), to see if the noise was method related. The results are presented in Figure 5, which shows that none of the methods has a definite advantage over the others and that noise is not method related.

The biggest variation along the segment occurs for the design #8. To eliminate any effect of optimization convergence, we optimized this configuration starting from the arithmetic mean of the optimal designs #7 and #9. This approach reduced the variation in the wing bending material weight for design #8 by about 5%.

Next, we investigated the effect of the aerodynamic loads by using the arithmetic mean of the loads from the cases of design #7 and design #9 as a starting point for optimization of design #8. This totally eliminated the variation, showing that the source of most of the noise arose from the loads that were applied to the structure. Figure 6, which shows the spanwise location of the center of pressure (CP) and of the inertia load center (IC) for the five load cases (LC), supports this conclusion. (The fifth load case is for taxiing, where only inertia loads are applied.)

Most of the curves have some variation at the design #8. The curve for the second load case (Mach number 2.4, load factor 1.0), which is critical, has the largest variation. In Ref. 13 it was shown that a change of 1.5 ft. in the spanwise location of the center of pressure can change the stresses in the wing by about 20%. This sensitivity of the stresses to the location of the center of pressure is due to the large amount of fuel carried in the wing of the HSCT. The inertia loads associated with the fuel cancel most of the aerodynamic loads, so that small changes in the aerodynamic loads can have large effects on the resultant bending moment. These changes in bending moments and stresses in turn have substantial effect on the results of the structural optimization.

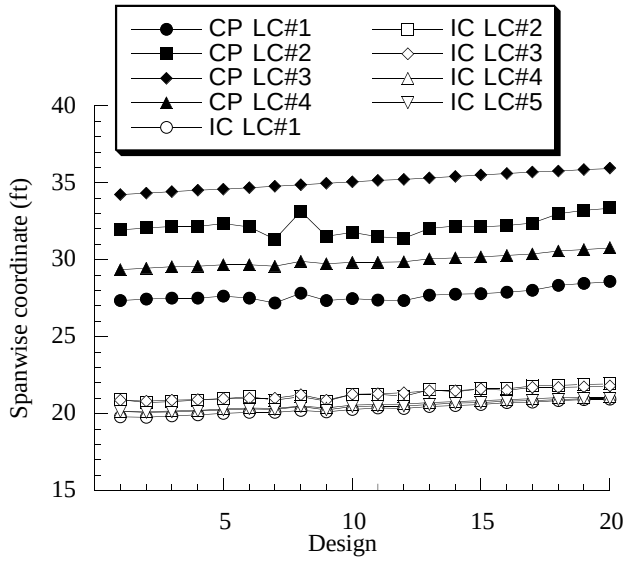

Figure 6. The spanwise coordinates of the center of pressure and of the inertia load center for 5 load cases. Cambered wing. (wing span is 81.9 ft.)

The variations in the inertia center location are mostly due to the fact that distribution of fuel between fuel tanks is optimized separately for each design[4]. Results of these independent optimizations are noisy, and they certainly effect the wing bending material weight calculations.

To further investigate the source of the noise in center of pressure location we studied the way camber is assigned to the wing. As mentioned earlier, camber is optimized by Carlson's program WINGDES which optimizes camber for each particular configuration. Apparently, the camber optimization can be noisy, too. Figure 7 shows the center of pressure and the inertia center locations for uncambered wing designs. The noise in the center of pressure location is totally eliminated.

These results indicate that a large portion of the noise in the wing bending material weight was due to separate optimization of the wing camber for each design. Furthermore, we found that the noise was mostly due to incomplete camber optimization. When we adjusted the optimization procedure, we improved the camber design at the cruise C_L and obtained much smoother wing camber as a function of wing geometry. That in turn significantly reduced amount of noise in the location of the center of pressure (Fig. 8). Due to different camber distribution, the center of pressure for all the cases moved outboard.

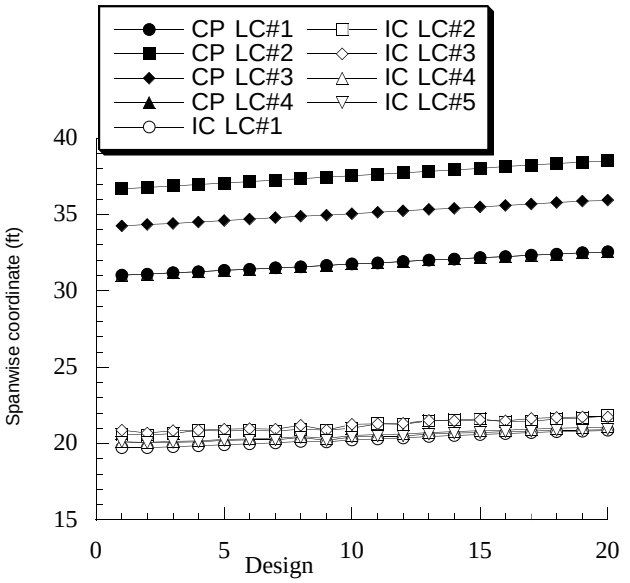

Figure 7. The spanwise coordinates of the center of presure and of the inertia load center for 5 load cases. Uncambered wing. (wing span is 81.9 ft.)

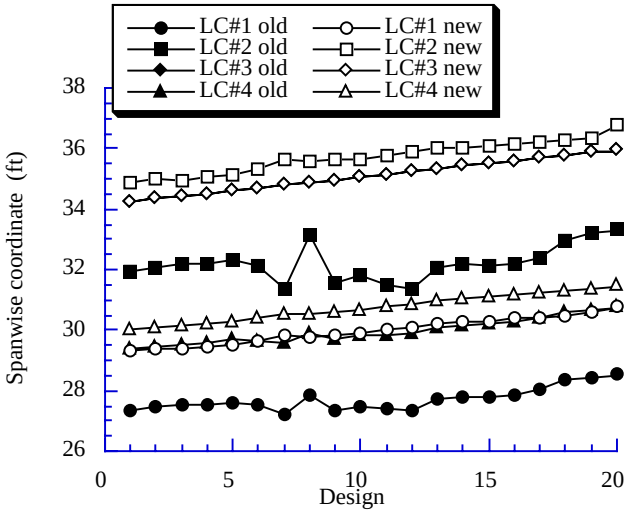

Figure 8. The spanwise coordinates of the center of presure for 4 load cases. Old and improved camber distribution. (wing span is 81.9 ft.)

After optimization of camber distribution was improved, we performed structural optimization for the designs of the α plot (Fig. 9). We obtained a significant reduction in the amount of noise in the results of the wing bending material weight. Most of the remaining noise could be attributed to incomplete convergence of the structural optimization, separate optimization of fuel redistribution for each design, and noise left in the locations of center of pressure and center of inertia. The significant "shift up" in the absolute values of the wing

bending material weight is due to significant changes in the spanwise coordinate of the center of pressure location. The remaining noise in our results will be filtered out by the response surface approximations. Figure 9 shows the results of one of the response surfaces, discussed later as RS1.

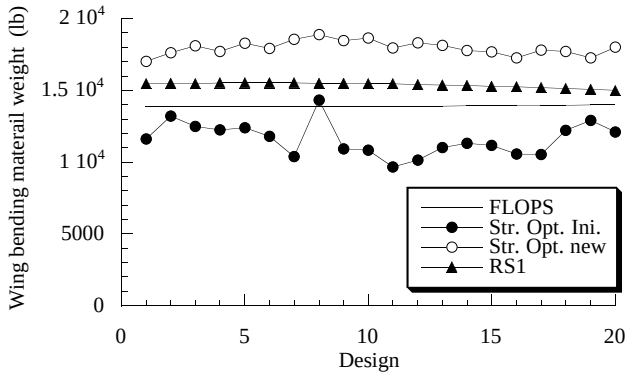

Figure 9. Wing bending material weight for the old and improved camber distribution.

6. Response Surface Approach

The response surface methodology (RSM) approach is not the only way of integrating structural optimization in the overall HSCT design process. For example, a multilevel decomposition approach was successfully used by Röhl *et al.*[14] and an interlacing factor approach was used by a design group at Virginia Tech[9]. A broad survey of methods is presented in Ref. 15. Currently, we employ RSM because it provides several attractive features not provided by other approaches. Particularly, it allows disciplinary codes to be executed by specialists *a priori* to overall design, rather than by generalists in the overall design process. RSM significantly simplifies multidisciplinary code integration and helps to filter out the noise in the response. Since the response surface is usually a low-order polynomial, the optimization task becomes computationally simple.

RSM is a statistical technique in which smooth functions, typically linear or quadratic polynomials, are used to model system response. In such a model the polynomial coefficients may be estimated using the method of least squares. To estimate the coefficients we need data at a certain number of points which is larger than the number of coefficients. Large ratios between the number of points and number of coefficients help filter out noise in the data as well as improve the fit of the polynomial to the response.

For the quadratic polynomial in p variables the number of terms in the model function, n, grows at a rate $\mathcal{O}(p^2)$. Creating a response surface for the n-term polynomial requires a number of points, N, which is larger than, but of the same order of magnitude as n. However, to maintain good accuracy, we would like the points where we use the response surface to be located within the convex hull of the data points used to construct the surface. To satisfy this for a p-dimensional box we must estimate response at 2^p points (at the vertices of the box). Such experimental design, when all the vertices of the p-dimensional box are evaluated, is called *full-factorial design* and denoted according to the number of the vertices evaluated (2^p). Another commonly used experimental design which includes only $2^{(p-m)}$ vertices of the p-dimensional box is called $2^{(p-m)}$ *fractional factorial design*[16]. For the twenty-eight design variables describing the HSCT, full-factorial design corresponds to more than 200 million points, which is certainly impossible to evaluate with present computational capabilities. This problem is often called the *curse of dimensionality*.

Another source of inaccuracy in the response surface is that quadratic polynomials cannot model well higher order variations. Also estimations outside the design space where the response surface was created may produce inaccurate results.

Several measures can be taken to address modeling error. First, the number of data points used to create the response surface can be increased so that the convex hull defined by the known data points encloses a larger portion of the design space. This option increases computational expense and we did not consider it for our high-dimensional problem. Second, the volume of the design space modeled by RSM could be reduced. This will lower the distance between points interior to the convex hull and the boundary of the convex hull. Another option is to reduce complexity of the model function by eliminating unnecessary terms. A statistical technique, analysis of variance[6] (ANOVA) enables the less significant terms in the polynomial approximation to be identified. Finally, the points can be selected so as to minimize modeling error.

Once the response surface is generated, its predictive capabilities must be evaluated. This is accomplished by finding the response surface prediction at a series of data points with known responses. Measuring the difference between the known and the predicted response yields the information including average error, root mean square (RMS) error[6], and maximum error.

6.1 Design of Experiments for Response Surface

Techniques for selecting analysis points in the design space is called design of experiments. RSM typically employs structured set of points such as central composite design (CCD)[17]. Consider the p-dimensional box centered at the origin of the system of coordinates. Then CCD represents vertices of this box, point at the center and $2p$ points at the axis of the system of coordinates, located symmetrically with respect to the center of the box. These $2p$ points are called axial points. However, CCD is only effective for a low dimensional regularly shaped design space, which is unlikely to appear in this study, where our design problem is described by 28 design variables. For an irregular design space in high dimensions, there is no simple way of creating a finite number of points that span the entire region. Hence, a very large number of points must be produced knowing that many will fall outside of the feasible design space. The infeasible points can then either be perturbed until they fall within the feasible region, or removed. This process will lead to a large number of points inside the feasible region, but whose geometric distribution is irregular. From these points, a small number must be chosen to construct the response surface.

In a previous study[18] it was found that the D-optimality criterion[19,6] provided a rational means for choosing the location of a given number of these points. This criterion seeks to minimize the variance in the coefficients of the response surface due to noise in the data. This is accomplished by maximizing the determinant of the normal equations used to obtain coefficients. The D-optimality criterion provides maximum protection against the effects of noise, but it is not well suited to handle modeling errors.

Another criterion, called minimum bias (ex., 20), seeks to minimize the modeling error (also called bias error) which reflects the fact that the function we use for the response surface (quadratic polynomial here) is different from the true response function. Myers and Montgomery[20] report on examples where minimum bias design sets of points had also good variance properties, but minimum variance sets of points did not have low bias properties.

To find a minimum bias set of points you have to postulate the true form of the approximated function. Since we employ a quadratic polynomial, we assume that the true wing bending material weight is a cubic polynomial. The minimum bias set of points satisfies the condition that

$$\frac{1}{V}\int_V m(x)dV = \frac{1}{N}\sum_{j=1}^{N} m(x_j) \ , \qquad (1)$$

where V is the volume of the reasonable design space, $m(x)$ is any monomial term obtained from multiplying a cubic polynomial by a quadratic polynomial, and N is the number of design points used for the response surface.

7. Variables for Wing Bending Material Weight Function

A response surface was created for the wing bending material weight by assuming a polynomial model equation and then estimating the polynomial coefficients using the method of least squares. We initially chose the variables to be twenty-five of the twenty-eight HSCT design variables (Table 1). The remaining three variables, the wing leading edge radius, the cruise climb rate and the starting cruise altitude were omitted because they had no effect on the wing bending material weight. For twenty-five variables, we have 351 coefficients which must be found through the method of least squares. However, to find these coefficients, large number of structural optimizations is required.

To reduce the number of coefficients we sought an alternative, smaller, set of variables (intervening variables), which would be more appropriate for a weight analysis while also being entirely dependent on the design variables. The intervening variables were chosen by analyzing the FLOPS equation for the wing bending material weight. It was found that the wing weight is based entirely on a set of ten basic parameters. Listed in Table 4, each of these parameters can be found using the twenty-five HSCT design variables. However, moving from these intervening variables back to original 28 design variables cannot be done easily.

Table 4. Parameters used to calculate wing weight in FLOPS.

Num.	Name	Description
1	S_{ht}	Horiz. tail area
6	B_{ze}	Engine relief factor
2	S_{vt}	Vert. tail area
7	B_z	Bending material fact.
3	D_{fuse}	Max. fuselage diam.
8	S_w	Wing surface area
4	b	Wing span
9	W_{fuel}	Takeoff fuel weight
5	$sweep$	Ave. 1/4 chord sweep
10	W_{to}	Gross weight from FLOPS

8. Identifying Reasonable Design Space

The main ingredient in customizing the weight function to the particular HSCT design requirements is to limit the design space to configurations that are reasonable for the design requirements. The first step in identifying the reasonable design space was to construct a suitably large hypercube, defined by the twenty-five

design variables (Table 1), that encompasses this entire region of space. Each of the variables, except the fuel weight, was allowed to assume values between 20% and 180% of its baseline value, given in Table 1. The fuel weight was only allowed to vary between 75% and 125% of its baseline value because of its strong influence on the design's range and therefore feasibility. 19,651 configurations were obtained by perturbing one, two and three variables at a time in such a way that perturbed variables reach their extreme allowable values. This technique is described in details in Ref. 6. Of the aircraft designs correspondent to these configurations, 83% violated one or more of the HSCT's geometric constraints (Table 2) and a large portion of the remaining designs appeared to be unreasonable.

Eliminating designs that are unreasonable could not be accomplished without removing nearly every design in the pool of 19,651 candidate points. For this reason, each unreasonable design $\mathbf{x}$ was moved so that it resided on the edge of the reasonable design space:

$$\mathbf{x}' = \alpha\,(\mathbf{x} - \mathbf{x}_c) + \mathbf{x}_c,\ \alpha > 0.$$

Computing α in the equation above required a set of criteria to determine whether a design was reasonable or not. These criteria were selected carefully to avoid a computationally expensive procedure and to ensure that no reasonable designs were inadvertently removed. To make use of complex constraints, a series of increasingly expensive evaluations were defined and applied in phases. Initially, the simple criteria were applied to the data and a large percentage of the candidate points were moved toward a nominal feasible point $\mathbf{x}_c$. However, as the increasingly complex constraints were applied, fewer of the points had to be moved and the expense of the constraint evaluations did not become prohibitive. Table 5 lists the criteria used to move the data towards the reasonable design space. They are listed in order of application, with the range constraint, which is the most expensive, coming last.

Table 5. Criteria for reasonable design.

Num.	Description
1-34	HSCT geometric constraints (Table 2)
35-36	20,000 lbs $< W_{b_F} <$ 120,000 lbs
37-58	Minimum fuselage radius
59	Inboard Λ_{le} > Outboard Λ_{le}
60	$\Lambda_{le} > 0$
61-62	5,000 ft^2 $< S_w <$ 15,000 ft^2
63-64	$1.0 < AR < 3.2$
65-83	$c_{y_{i+1}}/c_{y_i} < 1.0$
84	Approximate range > 5,000 n. mi.

In this table W_{b_F} is wing bending material weight computed by FLOPS, Λ_{le} - leading edge sweep angle, S_w - wing planform area, AR - aspect ratio, $c_{y_{i+1}}/c_{y_i}$ - local taper ratios.

9. Minimum Variance and Minimum Bias Response Surfaces

Due to the computational expense of the structural optimization, it was not possible to estimate wing bending material weight for all 19,651 points using structural optimization. It was necessary to choose points in the reasonable design space for creating the wing bending material weight response surface.

To create response surface that minimizes modeling error, we had to satisfy condition (1). This condition is difficult to satisfy for an irregular domain, and therefore we first transformed the domain to a 25-dimensional sphere. We scaled the design domain so that minimum and maximum values of each coordinate of all 19,651 points we had in the reasonable design space were assigned values -1 and 1, respectively. We also adjusted our domain to assure that points with only one coordinate equal -1 or 1 with the rest of the coordinates being zero had to correspond to reasonable aircraft design. With this criterion satisfied for extreme points, we ensure that our reasonable design space is close to sphere.

After we obtained the spherical domain, we selected the points in such a way that our experimental design satisfied equation (1). In a sphere, integrals of all monomials with any odd power are zero. One possible way to satisfy equation (1) is to construct a symmetric experimental design, so that all odd order monomial sums in (1) are zero. Even order monomials should satisfy the following conditions:

$$\sum_{j=1}^{N} {x_{i,j}}^2 = \frac{1}{N}\,\frac{1}{k+2}\ ,\ i = 1, \ldots, k$$

$$\sum_{j=1}^{N} {x_{i,j}}^4 = \frac{1}{N}\,\frac{3}{(k+2)(k+4)}\ ,\ i = 1, \ldots, k \qquad (2)$$

$$\sum_{j=1}^{N} {x_{i,j}}^2 {x_{r,j}}^2 = \frac{1}{N}\,\frac{1}{(k+2)(k+4)}\ , i \neq r\ ,$$

$$i, r = 1, \ldots, k$$

here k is the dimension of the problem (i.e., number of coordinates used), i, r are indices of particular coordinates, $x_{i,j}$ is the i coordinate of the j point in the design space. These conditions are described in detail in Ref. 21 and could be easily satisfied for low dimensional problems.

In our case of 25 variables, we selected a modified *small composite design*[22] that satisfied all the necessary requirements. While central composite design (CCD) includes full factorial design (all the vertices of the p-dimensional box) as a part, in small composite design

the full factorial portion is replaced by a fractional factorial portion. We employed a $2^{(25-15)}$ fractional factorial portion accounting for 1024 points. We also augmented our small composite design with additional 50 axial points for a total of 100 axial points. Including the central point, this experimental design consisted of 1125 points. The coordinates of the points in this experimental design were selected to satisfy criteria (2).

In low dimensions the minimum bias requirement causes the points to be located close to the center of the design space. However, in our high-dimensional case we obtained a design where all but 50 axial points were located very close to the surface of the sphere that bounded our design domain. This fact led us to hope that in addition to good bias properties our design would possess good variance properties also (experimental designs which minimize variance, consist of points that are usually located at the perimeter of the design space). Response surface in 25 design variables was constructed based on minimum bias experimental design.

It is also possible to create a minimum bias design in the 10-dimensional space of the intervening variables. However, while it is straightforward to calculate the intervening variables from the original variables, the opposite is not easy. We did not managed to find a good procedure to accomplish this inverse transformation. So, we have constructed a minimum bias response surface only for the 25-variable case.

We also considered minimum variance response surfaces which were based on the D-optimal experimental designs. The D-optimal set of points for the minimum variance designs was found by "k-exchange" method of Mitchell[23] as a subset of the original set of points. This procedure was used for the 25 design variables, and the resultant set was employed also for the 10-variable case.

The two minimum variance response surfaces are denoted RS1 (in 25 variables) and RS2 (in 10 intervening variables). The minimum bias response surface is denoted RS3. Each response surface is constructed based on 1125 points and checked based on additional 1,000 points selected based on D-optimality criterion. With RS1 and RS2 using the same data points, we performed a total of 3,250 structural optimizations

The approach used for creation of minimum variance response surfaces in this paper is the same as the approach used by Kaufman *et al.*[6]. However the structural optimization data used by Kaufman *et al.* was noisy. In our case we reduced the amount of noise considerably (see Fig. 9). The accuracy of the response surfaces in the current work is compared with similar models from Ref. 6 and the FLOPS weight function (Table 6).

Table 6. Comparison of RS Accuracy.

RS	Avg. Err.(%)	RMS Err.(%)	Max. Err.(%)
RS1 (25 dv, D-opt.)	4.29	6.61	71.08
RS2 (10 dv, D-opt.)	10.06	13.78	89.31
RS3 (25 dv, min. b.)	4.43	6.45	52.77
RS1* (25 dv, prev.)	7.72	12.78	114.58
RS2* (10 dv, prev.)	8.84	12.11	63.67
FLOPS	29.84	49.07	297.29

In this table RS1* refers to the response surface constructed by Kaufman *et al.* for standard 25 variables based on D-optimal points selection, RS2* refers to response surface constructed by Kaufman *et al.* for intervening variables based on the same set of points as RS1*, and FLOPS refers to the FLOPS weight function.

From Table 6 it is seen that all response surfaces have substantially lower errors than the FLOPS weight function. This reduced error is the consequence of customizing the response surfaces to the particular design conditions of the HSCT problem.

Comparing RS1 and RS2 to the more noisy results obtained with RS1* and RS2*, we see substantial improvement for the 25-variable RS1 and small degradation in the accuracy of the 10 intervening variables RS2. The improvement in RS1 reflects the reduced effect of the noise. For RS2, with 1,000 points used to calculate 66 coefficients, it is possible that the noise was already filtered out in RS2*, so that errors are mostly modeling errors. Comparing the minimum bias design RS3 to the minimum variance design RS1, we observe similar performance, indicating no advantage to one over the other.

Another effect of the reduced noise levels is in the number of polynomial coefficients that are characterized well by the data. Kaufman *et al.* found that only 61 coefficients out of 351 were retained for RS1* when ANOVA technique were employed to eliminate poorly characterized coefficients. Similarly, only 15 out of 66 coefficients were retained for RS2*. Here, in contrast, 163 coefficients were retained for RS1 and 52 for RS2. Model RS3 retained 81 coefficient.

10. HSCT Design Optimization

Complete HSCT design optimizations were performed to evaluate the effects of using the response surfaces to wing bending material weight, RS1, RS2 and RS3. At the completion of the optimizations, results were compared with structural optimization results. Implementation of each response surface was accomplished by modifying the gross takeoff weight calculations within the weight module of FLOPS. In place of FLOPS estimates for wing bending material weight, response surface predictions were used. RS1, RS2 and RS3 were intended for use in the reasonable design space and their predictions could not be relied

upon outside this region. Therefore, all calculations outside the reasonable design space were done with FLOPS. At the edge of the reasonable design space, a smoothing function was used to prevent discontinuity between wing bending material weight calculated by FLOPS and the response surface predictions[6].

Four HSCT configuration optimizations were performed, each starting from the baseline design detailed in Table 1. During the first optimization, the FLOPS wing bending material weight was used to find the take-off gross weight. The next three optimizations were performed using RS1, RS2 and RS3 respectively. Results from these optimizations are given in Table 7 and the planforms are plotted in Figures 10, 11, 12 and 13.

Table 7. Comparison of HSCT optimal designs.

Parameter	FLOPS	RS1	RS2	RS3
Planform Geometry				
Root chord (ft)	161.5	141.0	158.3	158.2
Tip chord (ft)	7.44	7.51	7.65	7.66
Wing semi-span (ft)	60.9	62.4	60.6	60.4
Aspect Ratio	1.74	1.84	1.79	1.76
Wing Area (ft^2)	10,263	10,160	9,927	10,049
Performance Data				
Range (n. mi.)	5,510	5,516	5,505	5,498
Landing AOA (°)	11.87	11.84	12.01	11.99
L/D max	8.98	9.16	8.91	8.92
Weight Data				
W_g (lbs)	622,551	622,439	618,168	620,488
W_b (lbs)	18,755	41,221	18,224	17,674
W_{b_G} (lbs)	22,848	36,767	21,517	20,244
W_f (lbs)	331,821	328,709	330,248	331,618

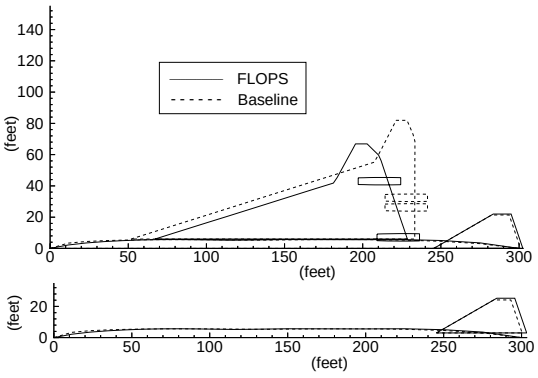

Figure 10. Optimal HSCT planform using FLOPS compared to baseline configuration.

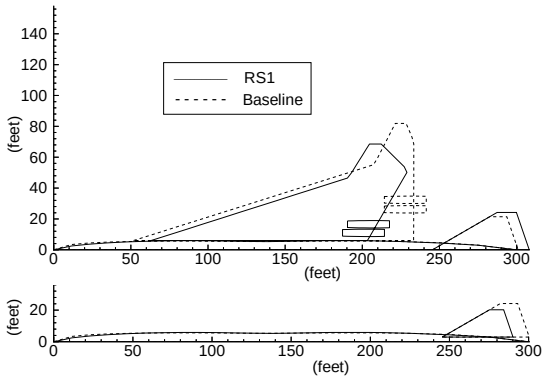

Figure 11. Optimal HSCT planforms using RS1 compared to baseline configuration.

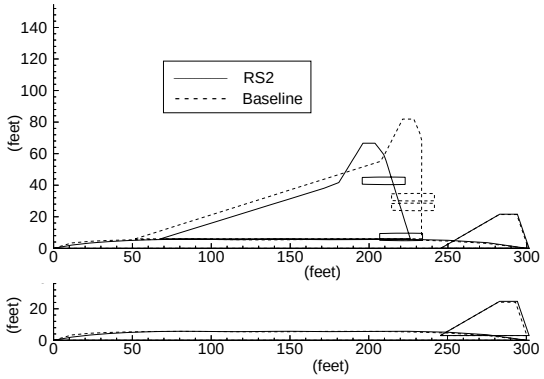

Figure 12. Optimal HSCT planforms using RS2 compared to baseline configuration.

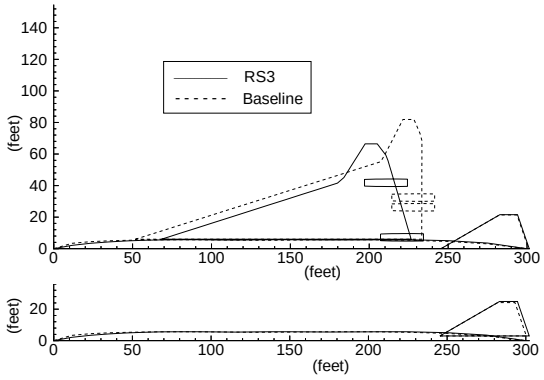

Figure 13. Optimal HSCT planforms using RS3 compared to baseline configuration.

In Table 7 W_g denotes gross weight, W_b denotes wing bending material weight calculated by correspondent response surface, W_{b_G} - wing bending material weight calculated by structural optimization with GENESIS, and W_f - required fuel weight.

Comparing the results in Table 7 and figures 10 - 13, we see that the optimizations using FLOPS, RS2 and RS3 obtained structurally efficient designs (low W_b)

which were less efficient aerodynamically (low L/D). The optimization using RS1 found an aerodynamically efficient design with high structural weight. The response surface errors in W_b at the optima are of similar relative magnitude, but because RS1 has a conservative error (it overestimates the weight) it probably corresponds to slightly superior design.

The error in the FLOPS estimate of W_b at the optimum is highest, but the difference is smaller than may be expected from Table 6. This may indicate that FLOPS works well for optimal designs since this weight equation was created based on actual aircraft data. Overall, the use of the response surface led to small improvement in performance compared to the use of FLOPS weight equation.

11. Concluding Remarks

When structural optimization is integrated into aircraft configuration optimization, the structural weight is inherently a non-smooth function of the configuration shape variables. Additional noise may be created due to noise in aerodynamic loads and incomplete convergence of the structural optimization. For our model of the HSCT, we have found noise of the order of 30% for the wing bending material weight obtained from structural optimization. A small part of this noise was eliminated by improving the convergence of the optimization procedure. Most of the noise however, was traced to noise in the aerodynamic loads. Careful implementation of camber optimization allowed us to reduce the amount of noise significantly.

To further smooth out the noise and facilitate the integration of the structural optimization in the overall design process we have explored the use of response surfaces for representing the optimum structural weight. The design points used for structural optimization for constructing the response surfaces were selected on the basis of the minimum variance and minimum bias criteria.

To ensure good accuracy of the response surfaces, simple analysis tools were employed. These tools were used to eliminate unfeasible regions of the design space, thus customizing the weight equation to aircraft with the given range, Mach number, etc. Additionally, the original FLOPS weight equation was used to identify important parameters for determining wing bending material weight, allowing a reduction in the number of variables from 25 to 10.

Optimizations of the HSCT configurations were conducted using 25-variable minimum bias and minimum variance response surfaces as well as 10-variable minimum variable response surface. These were compared to optimization based on the FLOPS weight equation. The application of the customized weight equation to configuration optimization of HSCT achieved superior design to that obtained by use of the original weight equation.

Acknowledgment

This work was supported by NASA Grants NAG-1-1562 and NAG-1-1160.

References

1. Hutchison, M. G., Mason, W. H., Grossman, B. and Haftka, R. T., "Aerodynamic Optimization of an HSCT Configuration Using Variable-Complexity Modeling", AIAA-93-0101, *31st Aerospace Sciences Meeting & Exhibit*, Reno, Nevada, January 11–14, 1993.
2. Hutchison, M., Unger, E., Mason, W., Grossman, B. and Haftka, R., "Variable-Complexity Aerodynamic Optimization of an HSCT Wing Using Structural Wing-Weight Equations", *Journal of Aircraft*, Vol. 31, No. 1, pp. 110-116, Jan.–Feb. 1994.
3.. McCullers, L. A., "Aircraft Configuration Optimization Including Optimized Flight Profiles", Proceedings of *Symposium on Recent Experiences in Multidisciplinary Analysis and Optimization*, J. Sobieski, compiler, NASA Cp–2327, April 1984, pp. 395–412.
4. Huang, X., Haftka, R. T., Grossman, B., and Mason, W., "Comparison of Statistical-based Weight Equations with Structural Optimization for Supersonic Transport Wings", AIAA 94–4379, 1994.
5. Vanderplaats, Miura and Associates, Inc., GENESIS User Manual, Version 1.3, Dec. 1993, 5960 Mandarin Avenue, Suite F, Goleta, CA 93117
6. Kaufman, M., Balabanov, V., Burgee, S., Giunta., A. A., Grossman, B., Mason, W. H., Watson, L. T., and Haftka, R. T., "Variable-Complexity Response Surface Approximations for Wing Structural Weight in HSCT Design", AIAA 96–0089, *34th Aerospace Sciences Meeting and Exhibit*, Reno, NV, January 15-18, 1996.
7. Balabanov, V., Kaufman, M., Giunta., A. A., Grossman, B., Mason, W. H., Watson, L. T.,and Haftka, R. T., "Developing Customized Wing Weight Function by Structural Optimization on Parallel Computers", AIAA 96–1336, Proceedings of the *37th AIAA/ASME/ASCE/AHS/ASC Structures, Structural Dynamics, and Materials Conference and Exhibit*, pp. 113–125, Salt Lake City, UT, April 15–17, 1996.
8. Carlson, Harry W. and Walkley, Kenneth B., "Numerical Methods and a Computer Program for Subsonic and Supersonic Aerodynamic Design and Analysis of Wings With Attainable Thrust Corrections," NASA CP 3808, 1984.

9. Dudley, J., Huang, X., MacMillin, P. E., Grossman, B., Haftka, R. T., and Mason, W. H., "Multidisciplinary Optimization of the High-Speed Civil Transport." AIAA 95–0124, *33rd Aerospace Sciences Meeting and Exhibit*, Reno, Nevada, January 9–12, 1995.
10. Hutchison, M. G., Unger, E. R., Mason, W. H., Grossman, B., and Haftka, R. T., "Aerodynamic Optimization of an HSCT Wing Using Variable-Complexity Modeling," AIAA Paper 93–0101, Jan. 1993.
11. Barthelemy, J. F. M., Wrenn, G. A., Dovi A. R., Coen, P. G., and Hall, L. E., "Supersonic Transport Wing Minimum Weight Design Integrating Aerodynamics and Structures," *J. of Aircraft*, Vol. 31, No. 2, March–April 1994.
12. Giunta. A. A, Narducci R., Burgee, S., Grossman, B., Mason, W. H., Watson, L. T. and Haftka, R. T., "Variable-Complexity Response Surface Aerodynamic Design of an HSCT Wing", AIAA 95–1886, Proceedings of *13th AIAA Applied Aerodynamics Conference*, San Diego, CA, June 19-22, 1995, pp. 994-1002.
13. Knill, D. L., Balabanov, V., Grossman, B., Mason, W. H. and Haftka, R. T., "Certification of a CFD code for High-Speed Civil Transport Design Optimization", AIAA 96–0330, *34th Aerospace Sciences Meeting and Exhibit*, Reno, NV, January 15-18, 1996.
14. Röhl, P. J., Mavris, D. N., Schrage, D. P., "HSCT Wing Design Trough Multilevel Decomposition", AIAA 95–3944, 1995.
15. Haftka, R. T., Sobieszczanski-Sobieski, J., "Multidisciplinary Aerospace Design Optimization: Survey of Recent Developments", AIAA 96–0711, *34th Aerospace Sciences Meeting and Exhibit*, Reno, NV, January 15-18, 1996.
16. Myers, R. H., Montgomery, D. C., "Response Surface Methodology. Process and Product Optimization Using Designed Experiments", *John Willey & Sons, Inc.*, New York, N. Y., 1995, pp. 134–174.
17. Mason, R. L., Gunst, R. F., and Hess, J. L., *Statistical Design and Analysis of Experiments*, John Wiley & Sons, New York, N. Y., 1989, pp. 215–221.
18. Giunta, A. A., Dudley, J. M., Narducci, R., Grossman, B., Haftka, R. T., Mason, W. H., and Watson, L. T., "Noisy Aerodynamic Response and Smooth Approximations in HSCT Design," AIAA Paper 94–4376, *5th AIAA/USAF/NASA/ISSMO Symposium on Multidisciplinary Analysis and Optimization*, Panama City Beach, Florida, September 7–9, 1994.
19. Box, M. J. and Draper, N. R., "Factorial Designs, the $|\mathbf{X}^T\mathbf{X}|$ Criterion, and Some Related Matters," *Technometrics,* Vol. 13, No. 4, 1971, pp. 731–742.
20. Myers, R. H., Montgomery, D. C., "Response Surface Methodology. Process and Product Optimization Using Designed Experiments", *John Willey & Sons, Inc.*, New York, N. Y., 1995, pp. 402–418.
21. Myers, R. H., "Response Surface Methodology", Blacksburg, VA, *published by Author*, 1976, pp. 202–214.
22. Myers, R. H., Montgomery, D. C., "Response Surface Methodology. Process and Product Optimization Using Designed Experiments", *John Willey & Sons, Inc.*, New York, N. Y., 1995, pp. 351–357.
23. Mitchell, T. J., "An Algorithm for the Construction of D-Optimal Experimental Designs", *Technometrics*, Vol. 16, No. 2, May 1974, pp. 203–210.